

Derivation and Validation of Mesoscopic Theories for Diffusion of Interacting Molecules

D. G. Vlachos^{1,*} and M. A. Katsoulakis^{2,†}

¹*Department of Chemical Engineering, University of Massachusetts Amherst, Amherst, Massachusetts 01003-3110*

²*Department of Mathematics and Statistics, University of Massachusetts Amherst, Amherst, Massachusetts 01003-3110*

(Received 31 March 2000)

A mesoscopic theory for diffusion of molecules interacting with a long-range potential is derived for Arrhenius microscopic dynamics. Gradient Monte Carlo simulations are presented on a one-dimensional lattice to assess the validity of the mesoscopic theory. Results are compared for Metropolis and Arrhenius microscopic dynamics. Non-Fickian behavior is demonstrated and it is shown that microscopic dynamics dictate the steady-state concentration profiles.

PACS numbers: 68.35.Fx, 02.70.Ns, 66.30.-h

Diffusion of interacting species (molecules or particles) is of fundamental importance in numerous applications ranging from colloids, to separations through membranes, to epitaxial growth, to catalytic reactors. Several of these processes operate far from equilibrium, where a macroscopic gradient is imposed or established across the system as shown schematically in Fig. 1(a). Under such conditions, gradients in concentration develop. The mass balance of a diffusing species is $c_t = -\nabla \cdot (-j)$, and the flux j through the system is often described by Fick's first law [1]

$$j = -D_F \nabla c = D_F^o (c_o - c_L) / L, \quad (1)$$

where D_F is the Fickian diffusivity, c is the concentration, t is the time, L is the system thickness, and D_F^o is the overall diffusion coefficient often determined experimentally from the overall concentration difference ($c_o - c_L$) and the flux measurement. Equation (1) is also referred to as a constitutive equation and is often an approximation of the underlying physics for interacting species. In particular, Fick's first law is structurally invalid when two phases coexist [2]. The latter case can lead to a physically unrealistic negative Fickian diffusion coefficient.

To handle such nonequilibrium problems at the molecular level, a dual control volume grand canonical molecular dynamics (DCV-GCMD) simulation approach was recently proposed and applied to numerous examples involving diffusion of a fluid [3–5] under a gradient in the chemical potential. Simulations under the conditions performed indicated small deviations from Fickian behavior that cannot be unambiguously discerned from the noisy MD data (e.g., [5]). Despite their parallel implementation, such simulations are limited to short length and time scales (e.g., several molecular diameters and nanoseconds). Practical systems such as membranes, on the other hand, are often several microns in thickness, and diffusion of slow moving molecules, through a hopping process, takes place over longer time scales.

Continuous time Monte Carlo (CTMC) simulations on a lattice (for a review in zeolites, see [6]) can only partially overcome this length-time scale problem. This difficulty can be circumvented by the development of a mesoscopic

transport theory. While such a theory has been proposed and studied for Metropolis/Kawasaki dynamics [7–9], no such theory exists for Arrhenius dynamics, which commonly occurs for site-to-site diffusion jumps of molecules on surfaces and in nanopores, and of vacancies and interstitials in solids. Inherent in the derivation of mesoscopic theories is the fact that the range of the intermolecular potential is infinite. In practice, however, many systems exhibit relatively short-range interactions, rendering quantitative application of mesoscopic theories uncertain. Currently, there has not been any quantitative validation of such mesoscopic theories.

Here we derive for the first time the underlying mesoscopic theory when diffusion follows Arrhenius microscopic dynamics. CTMC simulations are then outlined for Metropolis and Arrhenius dynamics on a one-dimensional lattice under a concentration gradient, as happens, for example, in permeation experiments through membranes. Such nonequilibrium conditions allow us to numerically assess for the first time the validity of mesoscopic theories as a function of the range of the intermolecular potential. Finally, comparison of results allows us to exploit whether it could be possible to discriminate different microscopic dynamics experimentally.

First we start with the derivation of the mesoscopic theory for Arrhenius diffusion dynamics, i.e., when the hopping probability depends on the activation energy between the initial state and the activated complex. This activation energy is here associated with the departing site x

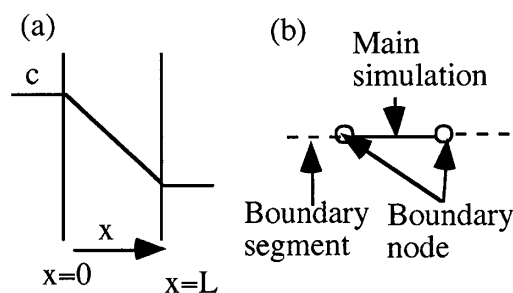


FIG. 1. Schematic of physical configuration (a) and simulation box (b).

(see [10–12] for an application of such Arrhenius dynamics in MC simulations of growth and surface processes). In particular, the diffusion rate of a particle located at the lattice site x that migrates to a neighboring empty site y is $v(x \rightarrow y) = d \exp[-\beta U(x)]$, where d is the diffusion and the energy $U(x)$ is associated with the long-range intermolecular potential of adsorbate-adsorbate interactions $J = J(x - y)$: $U(x) = U_o + \sum_{z \neq x} J(x - z)s(z)$. Here U_o is the energy associated with the binding to the site x , $s(z) = 0$ or 1 denotes the occupation number at the lattice site z , and $\beta = 1/kT$, where k is the Boltzmann constant and T is the temperature. Arrhenius dynamics satisfies detailed balance and differs from Metropolis or Kawasaki dynamics, whose hopping rate depends on the difference $U(x) - U(y)$. A more complex dependence of the activation energy on the energetics of adjacent sites is also possible and will be discussed elsewhere.

The mesoscopic theory is directly derived from the master equation as an evolution for the local coverage $Es_t(x)$ (or equivalently the probability of the site x being occupied) when the lattice size h vanishes; here E denotes the expectation with respect to the initial measure. We give a formal description of the derivation, whereas a mathematically rigorous proof obtained using the correlation function method will appear elsewhere. From the master equation we obtain $\partial_t Es_t(x) = \sum_{y \in N(x)} E[s_t(y) - s_t(x)]v(x \rightarrow y)$, where $N(x)$ denotes the nearest neighbors of x . When the interparticle potential is long range the fluctuations of $s_t(z)$ around their averages become independent, the law of large numbers formally applies, and $\sum_{z \neq x} J(x - z)s_t(z) \approx \sum_{z \neq x} J(x - z)Es_t(z)$. In addition, there is a normally distributed correction term of order $O(h^{k/2})$, in a k -dimensional lattice, due to the central limit theorem asymptotics. Rescaling time as $t \rightarrow th^{-2}$ and using the closure approximation $Es_t(x)s_t(y) \approx Es_t(x)Es_t(y)$, we obtain that as h vanishes, $Es_{th^{-2}}(x) \approx c(hx, t)$, and c solves in the continuum space (the potential length has to be small compared to the domain length)

$$c_t - \nabla \cdot \{De^{-\beta J * c}[\nabla c - \beta c(1 - c)\nabla J * c]\} = 0, \quad (2)$$

where $D = de^{-\beta U_o}$ and $J * c$ denotes the convolution. It is easy to see that c is also the probability density of the occupation number. We may also include the random fluctuations for the local coverage, in which case Eq. (2) becomes a stochastic PDE with the added random correction term $h^{k/2}\nabla \cdot \{[2De^{-\beta J * c}c(1 - c)]^{1/2}\dot{W}\}$. Here \dot{W} denotes a k -dimensional space/time white noise.

By introducing the free energy (note that r, r' denote points in continuum space, whereas x, y , and z denote lattice points)

$$E[c] = - \iint J(r - r')c(r)c(r')dr dr'/2 + \beta^{-1} \int [c \ln c + (1 - c) \ln(1 - c)]dr,$$

the flux can be written as $j = -\mu[c]\nabla(\delta E[c]/\delta c)$. Here the mobility term is *nonlocal* and given by $\mu[c] =$

$D\beta c(1 - c) \exp(-\beta J * c)$. In contrast, it was rigorously shown in [9] that for all diffusion dynamics where the migration rate depends on the energy difference, $U(x) - U(y)$, such as Kawasaki and Metropolis, the mobility is local and proportional to $c(1 - c)$. For such dynamics [9], the coverage on the lattice site x solves, as the lattice size h vanishes, the following mesoscopic equation

$$c_t - d\nabla \cdot \{[\nabla c - \beta c(1 - c)\nabla J * c]\} = 0. \quad (3)$$

According to Eqs. (2) and (3), the flux j for Arrhenius and Metropolis dynamics is, respectively,

$$j = -e^{-\beta J * c}D[\nabla c - \beta c(1 - c)\nabla J * c] \quad (4)$$

$$\text{and } j = -d[\nabla c - \beta c(1 - c)\nabla J * c].$$

Local stability analysis of uniform states of Eqs. (2) and (3) has also been performed. By considering a perturbation $\varepsilon e^{\omega t + i\xi x}$ to a uniform solution \bar{c} , the dispersion relation obtained for Arrhenius dynamics is $\omega = -|\xi|^2 De^{-\beta J_o}[1 - \beta \bar{c}(1 - \bar{c})\hat{J}(\xi)]$, where \hat{J} is the Fourier transform of J . The corresponding dispersion relation for Metropolis/Kawasaki dynamics lacks the Boltzmann factor (and has d instead of D), indicating that instabilities of uniform states during phase separation can grow much faster in this latter case.

A Taylor expansion in the concentration c gives that the convolution is $J * c = J_o c + J_2 \nabla^2 c + \dots$, where $J_o = \int J(r)dr$ and $J_2 = \int r^2 J(r)dr/2$ are the zero and second moments of the potential (note that we use the same notation for the discrete and continuum version of the energy U). When the concentration varies slowly (or in a suitable scaling regime [8]), then $U \approx J_o c$. Under such conditions, the flux can accurately be described by simplifying Eqs. (4), respectively, as

$$j \approx -e^{-\beta J_o c}D[1 - \beta J_o c(1 - c)]\nabla c \quad (5)$$

$$\text{and } j \approx -d[1 - \beta J_o c(1 - c)]\nabla c.$$

The prefactor of the concentration gradient shows the concentration dependence of an effective diffusion coefficient.

Next we describe the CTMC simulations. The main simulation box (line in 1D) has two boundary nodes and is augmented by two boundary segments of length equal to the potential range, as shown schematically in Fig. 1(b). Each boundary segment and boundary node represents a semi-infinite domain of prescribed concentration. Below simulations with boundary conditions $c_o = 1$ and $c_L = 0$ are reported since they establish the maximum possible gradient (far from equilibrium conditions). The total transition probability per unit time for the main simulation box is for Arrhenius and Metropolis dynamics, respectively:

$$\Gamma = \Gamma_o \sum_{\text{lattice}} e^{-\beta U_i} s_i (2 - s_{i+1} - s_{i-1}), \quad (6a)$$

$$\Gamma = \Gamma_o \sum_{\text{lattice}} s_i [P_{i \rightarrow i+1}(1 - s_{i+1}) + P_{i \rightarrow i-1}(1 - s_{i-1})], \quad (6b)$$

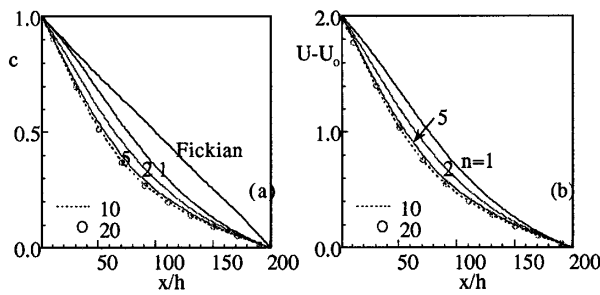


FIG. 2. Concentration (a) and energy (b) vs distance at various values of the intermolecular potential range n for Arrhenius dynamics and $\beta w = 1$.

where $P_{i \rightarrow j} = e^{-\beta(U_i - U_j)}$ when $U_j - U_i < 0$ and 1 otherwise (note that here $U > 0$ for attractive interactions). Here $2\Gamma_o$ is the total transition probability of jumping per unit time in the absence of interactions. When an event involves a boundary node, after the move the occupation function at the boundary node is instantly reset to its specified value. To properly compute the average lifetime of a lattice configuration, the summations restrict species at the boundary nodes to jump only into the main domain.

The execution of the algorithm proceeds as follows (a general introduction to the CTMC algorithm is given in [13]): The total transition probability per unit time is first computed, and a random number is used to select which atom (among the diffusing ones) will move. When there is only one empty adjacent site to the selected molecule, the hop takes place to this site. When both adjacent sites are empty, a second random number is used to decide the direction (left or right). This number is compared to the probability of one direction normalized by the sum of both directions (note that the transition probabilities to adjacent sites are generally different for Metropolis dynamics). Following a successful MC event, the time is incremented by an average expectation time of $1/\Gamma$. After steady state has been reached, the temporally averaged concentration and energy at each lattice point are computed for 10^6 MC steps.

In the limit of no interactions, random walk theory gives $d = 2\Gamma_o h^2/2$, where h is the lattice size. In the simulations reported, the parameters were chosen to be $h = 1$ and $\Gamma_o = 1$ (these values affect only the absolute value of j). For demonstration of ideas, the potential considered is

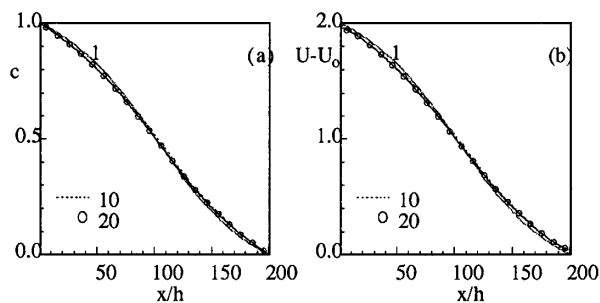


FIG. 3. Concentration (a) and energy (b) vs distance at various values of the intermolecular potential range n for Metropolis dynamics and $\beta w = 1$.

a step function, $J(x - y) = w/n$ when $|x - y| \leq n$ and $x \neq y$, and zero for longer distances. Here n denotes the range of the potential. For the discrete lattice case, n is the number of lattice points considered in determining the energy U . With this choice of potential, the convolution keeps the same value, for a uniform distribution of species as the range of the potential changes.

In the presence of attractive interactions considered here, a single-valued isotherm exists under equilibrium conditions for weak intermolecular potentials ($\beta w < 2$) [7,9]. In contrast, a bistable isotherm develops, within which spinodal decomposition is observed when $\beta w > 2$. The steady-state profiles obtained from CTMC for $\beta w = 1$ are shown in Figs. 2 and 3 for various values of the intermolecular potential range. For comparison purposes, the straight diagonal line in Fig. 2 represents the Fickian case ($w = 0$). It is seen that Arrhenius dynamics results in significant deviations from the Fickian behavior. As the range of the interactions increases, deviations rise and approach an asymptotic behavior at $n \sim 10-20$, where the differences in concentration are small to discern from the simulations. Figure 3 shows the corresponding results for Metropolis dynamics. Interestingly, both the concentration and energy profiles exhibit only small deviations from the Fickian case. Furthermore, it appears that the potential length is of secondary importance in affecting the concentration profile. Because of the significant difference in profiles between Arrhenius and Metropolis dynamics, measurement of steady-state concentration profiles, although difficult in many instances, can be used as a fingerprint of the microscopic dynamics. Such a large difference is solely caused by the Boltzmann factor in Eq. (2).

We now turn to the flux which is a quantity of practical interest. Figure 4 shows an example of the flux computed directly from the CTMC simulations by counting the number of molecules jumping via the interface between adjacent sites over a period of time. The steady-state flux is spatially constant throughout the domain with small noise. By smoothing the concentration and energy profiles, their derivatives are computed, and the components of the flux can be deduced, as shown in Fig. 4. As the potential range increases, the flux converges to an asymptotic value (mesoscopic behavior) that is practically achieved with a potential range greater than ~ 10 neighbors for Arrhenius

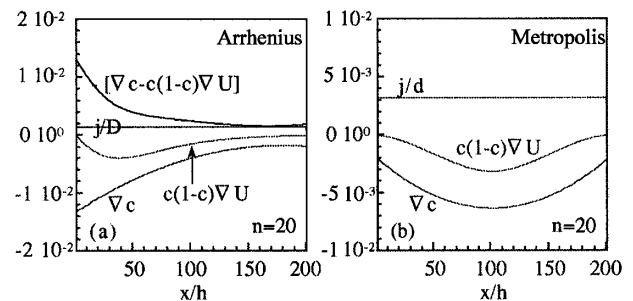


FIG. 4. Flux from CTMC simulations and its components for $\beta w = 1$.

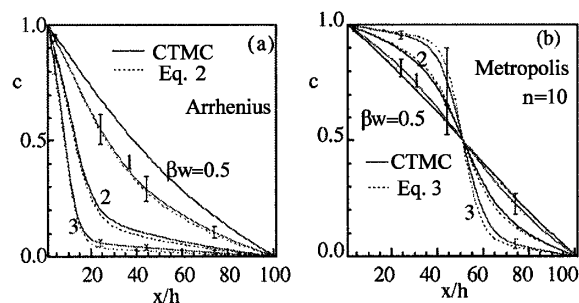


FIG. 5. Concentration vs distance from CTMC and the mesoscopic theories at various values of the intermolecular potential strength. The error bars indicate the standard deviation in MC results at selected spatial locations.

dynamics and ~ 20 for Metropolis dynamics. Note that due to subtractive contributions of concentration and energy gradients, overall the flux is only weakly sensitive on the intermolecular potential range (up to a few percent difference in flux from the asymptotic value is found even for $n = 1$).

With an asymptotic value of n identified, next in Fig. 5 we compare the steady-state solution of the mesoscopic Eqs. (2) and (3), solved using a second-order finite difference scheme, with the CTMC for various values of the potential strength w . The observed deviations in concentration and energy (not shown) are small for both types of microscopic dynamics. Up to $\sim 10\%$ deviation between the mesoscopically and molecularly computed fluxes has been found for all βw , despite the large concentration gradients within the spinodal decomposition regime ($\beta w \geq 2$).

Attractive interactions reduce the actual flux compared to the Fickian case. As a result, the overall diffusion coefficient D_F^o can be significantly lower than the Fickian one. For example, $d/D_F^o \sim 1.5$ (Metropolis) and $D/D_F^o \sim 3.3$ (Arrhenius) for $\beta w = 1$, and $d/D_F^o \sim 8$ (Metropolis) and $D/D_F^o \sim 25$ (Arrhenius) for $\beta w = 3$. Thus, in the presence of strong attractive intermolecular forces, the diffusivity can be significantly underestimated when interactions are ignored in the analysis of experimental data. A plot of D_F^o/D vs βw in Fig. 6 shows that only Arrhenius microscopic dynamics leads to a real Arrhenius behavior. Metropolis dynamics can, however, be fitted with an Arrhenius plot over a relatively narrow temperature range.

In summary, we derived a mesoscopic equation when the microscopic dynamics follows Arrhenius behavior. Gradient Monte Carlo simulations were performed for Arrhenius and Metropolis dynamics. It was found that the mesoscopic theory describes quantitatively the concentration and energy profiles for potentials with relatively short interaction range. The flux is described accurately even for first nearest-neighbor interactions. Finally, macroscopic concentration profiles are a distinct fingerprint, and could allow for experimental discrimination, of the microscopic dynamics. The mesoscopic Eq. (2) is valid

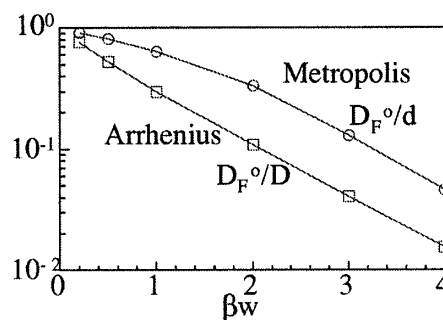


FIG. 6. Arrhenius graph.

in k dimensions. Our choice for 1D MC simulations was primarily motivated by our asymptotics which show that the stochastic correction to the mesoscopic equation is $O(h^{k/2})$, i.e., the worst-case scenario is the 1D. In fact, 2D simulations even with first nearest neighbors show similar concentration profiles, but improved agreement when compared to the mesoscopic theory. These dimensionality aspects will be discussed in detail in a forthcoming publication.

The research of M.A.K. and D.G.V. is partially supported by the National Science Foundation through DMS-9626904, DMS-9801769, CTS-9702615, CTS-9904242, and NETI. D.G.V. acknowledges the hospitality of the chemical engineering department at Princeton University during his sabbatical stay.

*Present address: Department of Chemical Engineering, University of Delaware, Newark, DE 19716-3110.

†Corresponding author.

- [1] R. B. Bird, W. E. Stewart, and E. N. Lightfoot, *Transport Phenomena* (Wiley, New York, 1960).
- [2] J. W. Cahn and J. E. Hilliard, *J. Chem. Phys.* **28**, 258 (1958).
- [3] G. S. Heffelfinger and F. van Swol, *J. Chem. Phys.* **100**, 7548 (1994).
- [4] J. M. D. MacElroy, *J. Chem. Phys.* **101**, 5274 (1994).
- [5] R. F. Cracknell, D. Nicholson, and N. Quirke, *Phys. Rev. Lett.* **74**, 2463 (1995).
- [6] S. M. Auerbach, *Int. Rev. Phys. Chem.* **19**, 155 (2000).
- [7] M. Hildebrand and A. S. Mikhailov, *J. Phys. Chem.* **100**, 19089 (1996).
- [8] M. A. Katsoulakis and D. G. Vlachos, *Phys. Rev. Lett.* **84**, 1511 (2000).
- [9] G. Giacomin and J. L. Lebowitz, *J. Stat. Phys.* **87**, 37 (1997).
- [10] G. H. Gilmer and P. Bennema, *J. Appl. Phys.* **43**, 1347 (1972).
- [11] D. G. Vlachos, L. D. Schmidt, and R. Aris, *J. Chem. Phys.* **93**, 8306 (1990).
- [12] D. D. Vvedensky, A. Zangwill, C. N. Luse, and M. R. Wilby, *Phys. Rev. E* **48**, 852 (1993).
- [13] A. B. Bortz, M. H. Kalos, and J. L. Lebowitz, *J. Comput. Phys.* **17**, 10 (1975).